ACS chemical biology

Articles

pubs.acs.org/acschemicalbiology

2-Hydroxyisoquinoline-1,3(2*H*,4*H*)-diones (HIDs), Novel Inhibitors of HIV Integrase with a High Barrier to Resistance

Belete A. Desimmie,[†,∥] Jonas Demeulemeester,[†,∥] Virginie Suchaud,[‡,⊥] Oliver Taltynov,[†,⊥] Muriel Billamboz,[‡] Cedric Lion,[‡] Fabrice Bailly,[‡] Sergei V. Strelkov,[§] Zeger Debyser,[†] Philippe Cotelle,[‡] and Frauke Christ*[,†]

[†]Molecular Virology and Gene Therapy and [§]Laboratory for Biocrystallography, KU Leuven, Department of Pharmaceutical and Pharmacological Sciences, Leuven, Belgium

[‡]Chimie Moléculaire et Formulation, EA 4478, Université de Lille 1, Villeneuve d'Ascq, France

Supporting Information

ABSTRACT: Clinical HIV-1 integrase (IN) strand transfer inhibitors (INSTIs) potently inhibit viral replication with a dramatic drop in viral load. However, the emergence of resistance to these drugs underscores the need to develop next-generation IN catalytic site inhibitors with improved resistance profiles. Here, we present a novel candidate IN inhibitor, MB-76, a 2-hydroxyisoquinoline-1,3(2*H*,4*H*)-dione (HID) derivative. MB-76 potently blocks HIV integration and is active against a panel of wild-type as well as raltegravir-resistant HIV-1 variants. The lack of cross-resistance with other INSTIs and the absence of resistance selection in cell culture indicate the potential of HID derivatives compared to previous INSTIs. A crystal structure of MB-76 bound to the wild-type prototype foamy virus intasome reveals an overall binding mode similar to that of INSTIs. Its compact scaffold displays all three Mg^{2+} chelating oxygen atoms from a single ring, ensuring that the only direct contacts with IN are the invariant P214 and Q215 residues of PFV IN (P145 and Q146 for HIV-1 IN, respectively), which may partially explain the difficulty of selecting replicating resistant variants. Moreover, the extended, dolutegravir-like linker connecting the MB-76 metal chelating core and *p*-fluorobenzyl group can provide additional flexibility in the perturbed active sites of raltegravir-resistant INs. The compound identified represents a potential candidate for further (pre)clinical development as next-generation HIV IN catalytic site inhibitor.

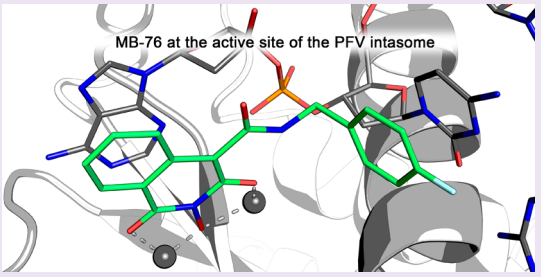

Since the first cases of acquired immune deficiency syndrome (AIDS) in 1981, more than 30 million people have fallen victim worldwide. Despite the enormous efforts put into developing new effective antivirals and the introduction of highly active antiretroviral therapy (HAART), only 8 out of more than 15 million eligible HIV-infected people are receiving treatment to date. The quest for novel antivirals complementing existing treatment options and active against the growing number of drug-resistant strains remains an important goal for present-day antiviral drug discovery. Next to the classical drugs targeting the viral enzymes reverse transcriptase (RT) and protease, raltegravir (RAL, MK-0518), which targets the strand transfer reaction of viral integrase (IN), was approved in 2007 for clinical use.[1] IN plays a crucial role in establishing irreversible infection by inserting the viral cDNA into host chromatin in two consecutive reactions.[2] First IN removes a GT dinucleotide from the 3′ end of the viral cDNA long terminal repeats (LTRs) (3′-processing, 3P). The viral preintegration complex (PIC) then passes through the nuclear pore into the nucleus.[3] Next, IN catalyzes the strand transfer (ST) reaction, introducing the viral cDNA ends 5 bp apart into host chromatin regions associated with active transcription.[4,5] For integration at these sites, HIV relies on the cellular chromatin tethering factor, LEDGF/p75 (ref 6 and references therein).

Approval of the first integrase strand transfer inhibitor (INSTI), RAL, in 2007[1] has validated the integration step as a target for antiretroviral therapy. Inhibition of integration by RAL is accompanied by an extremely rapid and strong reduction in viral load.[7] However, resistance evolves readily in the clinic,[8] necessitating the efforts to develop second-generation integrase inhibitors. Although elvitegravir (ELV, GS-9137) can be given once daily when combined with a booster (as part of the fixed-dose combination tablet Stribild), cross-resistance rules out treatment of patients failing on RAL therapy.[9,10] Dolutegravir (DTG, S/GSK1349572), an INSTI in phase III clinical trials, has some superior characteristics such as once daily dosing and a resistance profile only partially overlapping with that of RAL.[11−13] The recent determination of the prototype foamy virus (PFV) IN crystal structures in complex with viral DNA ends (the intasome) as well as various inhibitors has provided insight into the active site of IN, the

Received: January 18, 2013
Accepted: March 21, 2013
Published: March 21, 2013

Table 1. Activities of MB76 *in Vitro* and in Cell Culture

	overall[a,b]	ST[a,c]	3P[a,d]	EC_{50}[a,e]	CC_{50}[a,f]	SI[a,g]	BaL EC_{50}[a,i]	IIIB EC_{50}[a,j]
MB-76	0.056 ± 0.021	0.099 ± 0.041	0.066 ± 0.016	2.34 ± 0.24	>125	>53	0.257 ± 0.19	0.458 ± 0.399
RAL[h]	0.042 ± 0.013	0.047 ± 0.032	9.9 ± 5.1	0.007 ± 0.002	137.05 ± 11.19	18273	0.005 ± 0.004	0.004 ± 0.002

[a]In μM. [b]Concentration required to inhibit the IN overall catalytic activity *in vitro* by 50%. [c]Concentration required to inhibit the strand transfer *in vitro* by 50%. [d]Concentration required to inhibit the 3′ processing *in vitro* by 50%. [e]Effective concentration required to reduce HIV-1 induced cytopathic effect by 50% in MT-4 cells. [f]Cytotoxic concentration reducing MT-4 cell viability by 50%. [g]Selectivity index: ratio CC_{50}/EC_{50}. [h]Raltegravir. [i]Effective concentration required to reduce HIV-1 BaL induced cytopathic effect by 50% in peripheral blood mononuclear cells. [j]Effective concentration required to reduce HIV-1 IIIB induced cytopathic effect by 50% in peripheral blood mononuclear cells.

Table 2. Antiviral activity of MB-76, RAL, and AZT against Multiple Strains of HIV-1, HIV-2, and SIV

		MB-76[a]	RAL[a]	AZT[a]
HIV-1	Clade A	1.01 ± 0.07	0.0034 ± 0.0029	0.0175 ± 0.0026
	Clade D	1.77 ± 0.48	0.0095 ± 0.0031	0.0200 ± 0.0089
	Clade E	2.37 ± 2.04	0.0106 ± 0.0003	0.1206 ± 0.0037
	Clade F	1.22 ± 0.39	0.0055 ± 0.0014	0.0318 ± 0.0036
HIV-2	EHO	2.24 ± 1.05	0.0070 ± 0.0023	0.0022 ± 0.0020
	ROD	4.64 ± 2.77	0.0063 ± 0.0012	0.0045 ± 0.0015
SIV	Mac251	5.10 ± 2.50	0.0079 ± 0.0020	0.0036 ± 0.0024

[a]EC_{50} in μM. Effective concentration required to reduce virus-induced cytopathic effect by 50% in MT-4 cells.

INSTI mechanism of action, and the signature resistance development pathways.[14−16]

Against this background we now developed a novel class of integrase inhibitors, the 2-hydroxyisoquinoline-1,3(2*H*,4*H*)-diones (HIDs) (Supplementary Figure S1A,B) characterized by a high genetic barrier toward resistance development and a favorable cross-resistance profile with RAL. In addition, HIDs are potent inhibitors of both ST and 3P activities. By soaking a HID (MB-76) into PFV intasome crystals we corroborate their binding into the active site of IN and provide insight into the features that set HIDs apart from other INSTIs, in particular their high barrier toward resistance selection. A first ADMETox study demonstrates that HIDs do not induce any significant cellular toxicity and hardly inhibit the classical cytochrome P450 pathways. Detailed mechanism of action studies of HID/MB-76 support the potential for further clinical development of potent congeners.

RESULTS AND DISCUSSION

MB-76 Inhibits the Catalytic Activity of IN and Blocks HIV Replication. We first evaluated the effect of MB-76 on the 3P and ST activities of HIV-1 IN. Classical INSTIs such as RAL and ELV specifically inhibit ST, whereas inhibition of the 3P activity is at least 1 log lower.[17] Surprisingly, MB-76 showed equipotent inhibition of both reactions (IC_{50} = 66 ± 16 nM for 3P and IC_{50} = 99 ± 41 nM for ST) (Table 1). As the HID scaffold has previously been reported to inhibit the HIV-1 RT RNase H activity, we also determined the IC_{50} of MB-76 against this target.[18,19] With an IC_{50} of 0.36 μM, the RT RNase H is significantly less inhibited than IN, yet this may constitute a side activity of the compound. In cell culture MB-76 is active at low micromolar concentrations (EC_{50} = 2.34 ± 0.24 μM), a discrepancy with its *in vitro* potency that may be explained by low cell permeability (despite a cLogP value of 2.7) or high protein binding of the compounds. This issue is currently being addressed through pharmacomodulation. Since MB-76 did not induce any apparent toxicity (CC_{50} >125 μM), a favorable selectivity index >53 was reached (Table 1), allowing antiviral profiling of MB-76. To evaluate the potential of MB-76 to proceed from bench to bedside, we determined its antiviral activity in peripheral blood mononuclear cells (PBMCs) from healthy human donors (Table 1). MB-76 retained antiviral activity in these primary cells. Moreover the compound proved to be active against viral strains using either the CXCR4 (IIIB) or CCR5 (BaL) chemokine coreceptor. As with RAL we observed a higher activity in PBMCs with both the CCR5 (BaL) and CXCR4 (IIIB) specific viral strains (Table 1).

Considering the broad genetic diversity of HIV-1 and the variable prevalence of subtypes in the different regions of the world, we further investigated the anti-HIV activity of MB-76 against a spectrum of subtypes (clades A, D, E, and F; Table 2), including the most prevalent strains infecting patients in Europe, Africa, and Asia. Both MB-76 and RAL potently inhibit the complete spectrum of isolates tested, and no significant variation in activity of MB-76 was observed. Furthermore MB-76 inhibits the HIV-2 strains EHO and ROD and the macaque specific SIV strain Mac251, demonstrating that this novel class of IN catalytic site inhibitors inhibits HIV-1, HIV-2, and SIV.

MB-76 Blocks HIV Replication at the Step of Integration. To unambiguously attribute a novel antiviral activity to inhibition of a specific step in the HIV replication cycle, a thorough analysis of the mode of action in cell culture is required.[20] Next to cross-resistance profiling, Q-PCR and time-of-addition (TOA) experiments provide valuable insights. For the Q-PCR anaylsis, HeLaP4 cells were infected with HIV-1 IIIB in the presence of zidovudine (AZT), RAL, or MB-76. All three compounds strongly inhibited viral replication (Figure 1A). Reverse transcription of the viral RNA was blocked by AZT but not by RAL or MB-76, ruling out potent inhibition of the RT RNase H by MB-76 during viral replication (Figure 1B). In contrast, both RAL and MB-76 caused an approximately 7-fold increase in the number of 2-LTR circles (Figure 1C), a specific hallmark of IN inhibition.[21,22] All three drugs reduced viral integration to background levels (Figure 1D). TOA experiments have been widely used to pinpoint the stage of the HIV life cycle that is inhibited by antiretroviral compounds.[23] Here, we profiled MB-76 together with a set of established HIV replication inhibitors (Figure 1E). The compounds were added at different time points after infection of MT-4 cells with HIV-1 IIIB, and p24 antigen production in

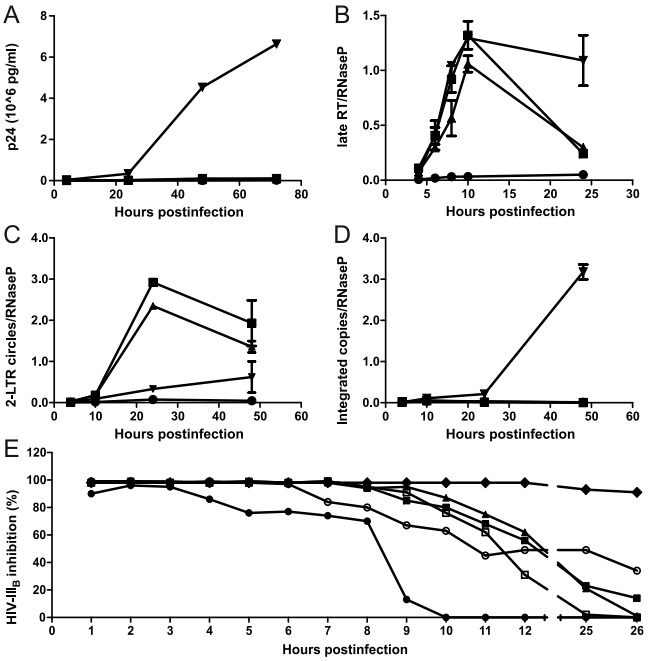

Figure 1. Analysis of the mechanism of action of MB76. (A–D) Q-PCR analyses of HIV-1 DNA species in single-round replication. Compounds were added at 50-fold EC_{50}. ▼, no inhibitor control; ▲, 100 μM MB-76; ■, 0.3 μM RAL; ●, 1 μM AZT. A representative experiment with duplicate measurements and SD is shown. (A) Inhibition of HIV-1 replication during the time course of the experiment as determined by p24 measurements. (B) Analysis of late RT transcripts. As expected, only AZT inhibits cDNA synthesis. (C) Analysis of 2-LTR circle formation as a measure of the block of integration. Both integrase inhibitors, MB-76 and RAL, induce a similar increase in 2-LTR circle formation. After 48h, second-round replication in the non-inhibited control results in an increased number of 2-LTR circles. (D) Analysis of the integration event. MB-76, RAL, and AZT reduce integration to background levels. (E) Time-of-addition (TOA) experiment. After infection of MT-4 cells with HIV-1 IIIB, inhibitors (50-fold EC_{50}) were added at indicated time points spanning from 1 to 26 h postinfection. ▲, MB-76; ■, RAL; □, ELV; ●, AZT; ○, efavirenz; ♦, saquinavir. Virus replication was determined by p24 antigen determination in the supernatant at 30 h postinfection. Relative inhibition (%) compared to the non-inhibited replication control is plotted. For comparison, RT inhibitors AZT and efavirenz were included, as well as INSTIs RAL and ELV, but also an inhibitor of late replication steps, the protease inhibitor saquinavir. MB-76 loses its inhibitory capacity if added later than 9 h postinfection, matching the profile observed for the INSTIs.

the supernatants was measured at 30 h postinfection. The antiviral activities of the RT inhibitor AZT started to diminish when added 4–5 h postinfection, whereas the loss of activity of efavirenz was delayed to 7 h postinfection. The activity of the protease inhibitor saquinavir dropped off slightly at 25 h after infection (Figure 1E). The activity of MB-76 started to diminish when added 7–8 h after infection, a profile similar to that of RAL and ELV. Both Q-PCR and TOA analyses indicate that, akin to the INSTIs RAL and ELV, MB-76 specifically targets HIV integration and not RNase H during viral replication.

MB-76 Retains Activity against RAL-Resistant Viruses. It is important that novel IN inhibitors have a high genetic barrier to resistance development and a favorable cross-resistance profile with current INSTIs. Therefore, we analyzed the cross-resistance profile of MB-76 in comparison with RAL and ELV but also with the nucleoside and non-nucleoside RT inhibitors AZT and efavirenz, respectively, and the CXCR4 inhibitor AMD3100 (Table 3).[21,24–28] As expected MB-76 possesses wild type activity against RTMC (AZT-resistant), A17 IIIB (efavirenz-resistant), and NL4.3/AMD3100 (AMD3100-resistant) strains, whereas resistance to all three respective drugs was indeed confirmed. Interestingly, although MB-76 potently inhibits the strand transfer reaction of IN, it retained full activity against all common INSTI-resistant strains tested (E92Q, Q148H, N155H, and G140S/Q148H), indicating a lack of cross-resistance with first-generation INSTIs and encouraging further clinical development. Especially the lack of cross-resistance with G140S/Q148H is a relevant finding, as these substitutions do still affect the activity of DTG, a second-generation INSTI in phase III clinical trials.[11–13] Of note, during the preparation of this manuscript, Métifiot et al. published a series of dihydro-1*H*-isoindole derivatives, the most potent of which (XZ-259) shows activity comparable to that of RAL.[29] This compound maintained its activity against Y143R-carrying RAL-resistant virus but did not inhibit strains with the clinically relevant N155H or G140S/Q148H substitutions.[29]

In order to assess the genetic barrier for resistance development to MB-76, we performed *in vitro* resistance selection (Figure 2A). As HIV rapidly evolves, any given antiviral drug so far has selected resistant strains, limiting its efficacy.[30] Accordingly, we carried out *in vitro* resistance selection in C8166 and MT-4 cells by gradually increasing the selective pressure of MB-76. However, when attempting to increase the concentration of MB-76 by 2-fold or more during the selection experiment, the virus failed to replicate. Even after 20 passages, the MB-76 concentration was only 4-fold above its

Table 3. Cross Resistance (Fold Change in EC_{50}) of MB-76 with other ARVs

		integrase			reverse transcriptase		
resistance	virus strain	MB76	RAL	ELV	AZT	EFV[a]	AMD3100
LEDGIN	A128T[b]	2	1	1	1	1	1
RAL	E92Q[c]	1	**5**	**6**	3	1	1
	Q148H[c]	1	**9**	1	2	1	1
	N155H[c]	1	**5**	3	2	1	1
	G140S/Q148H[c]	1	**486**	**154**	2	1	1
AZT	RTMC[d]	1	1	1	**18**	1	1
EFV[a]	A17RIIIB[e]	1	1	1	1	**23**	1
AMD3100	NL4.3/AMD3100[f]	2	2	1	3	1	**3260**

[a]Efavirenz. [b]HIV-1 strain selected to be resistant against LEDGINs.[19,22] [c]RAL (ref 23 and references therein). [d]NRTIs.[24] [e]NNRTIs.[25] [f]AMD3100.[26] The average values of at least 3 independent experiments are shown.

dx.doi.org/10.1021/cb4000426 | *ACS Chem. Biol.* 2013, 8, 1187–1194

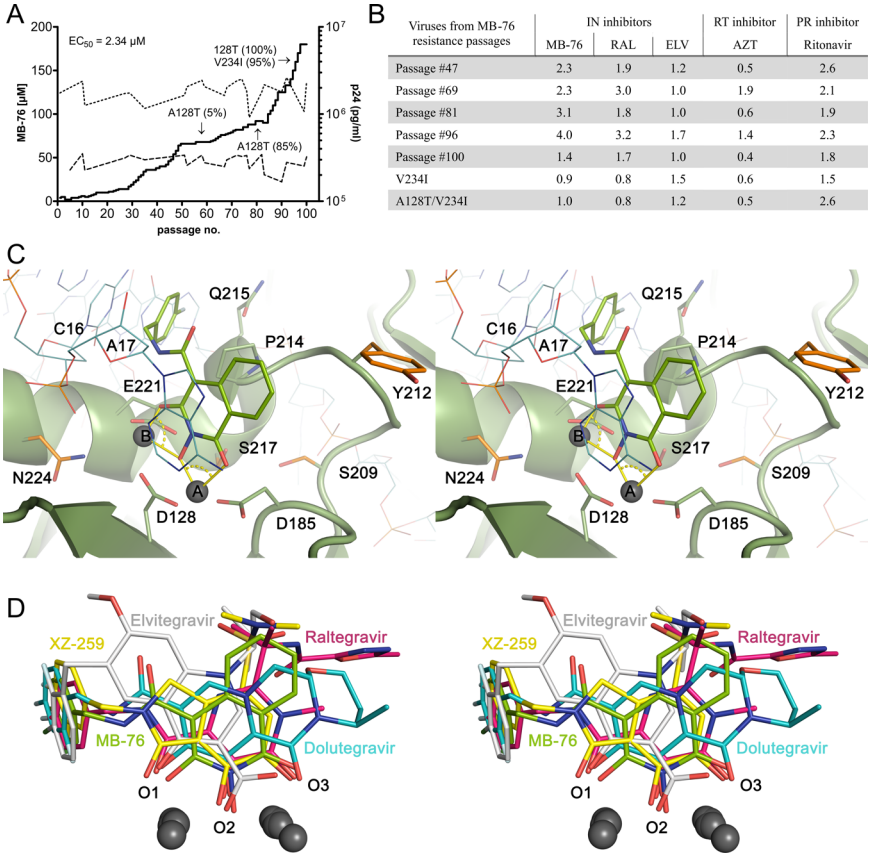

Viruses from MB-76 resistance passages	IN inhibitors			RT inhibitor	PR inhibitor
	MB-76	RAL	ELV	AZT	Ritonavir
Passage #47	2.3	1.9	1.2	0.5	2.6
Passage #69	2.3	3.0	1.0	1.9	2.1
Passage #81	3.1	1.8	1.0	0.6	1.9
Passage #96	4.0	3.2	1.7	1.4	2.3
Passage #100	1.4	1.7	1.0	0.4	1.8
V234I	0.9	0.8	1.5	0.6	1.5
A128T/V234I	1.0	0.8	1.2	0.5	2.6

Figure 2. Resistance selection and structural analysis of MB-76 binding to the catalytic site of the PFV-intasome. (A) Long-term resistance selection on wild-type HIV-1 NL4.3 in MT-4 cells with escalating concentrations of MB-76 (full line, plotted on the left *y*-axis). HIV cytopathic effect was followed, and p24 production in the supernatant for the control and MB-76 (dotted and dashed lines respectively) is plotted on the right *y*-axis. Sequencing results for IN-coding regions at passage 57, 81, 96, and 100 identified A128T and V234I mutations and are shown at the indicated passages. Percentages derive from population sequencing and are relative to the control. (B) Phenotypic resistance (fold change in EC_{50}) of viruses grown in the presence of MB-76 (panel A) against MB-76 itself, RAL, ELV, AZT, or ritonavir. All test compounds are active against the viruses from the different passages and the molecular clones of the mutations identified in the IN-coding regions. (C) Stereoimage of MB-76 (sticks) bound at the DNA–protein interface in the PFV intasome active site, as determined by X-ray diffraction. The two catalytic Mg^{2+} ions (A and B) are held in place by DDE signature residues D128, D185, and E221. MB-76 has displaced the 3′-terminal deoxyribose from the Mg^{2+} B coordination sphere, and its *p*-fluorobenzyl group now occupies the site where the adenine base is normally located. This base is now observed to stack against the HID core. PFV IN residues S209, Y212, S217, and N224 are shown in orange sticks and correspond to HIV G140, Y143, Q148, and N155, respectively. These positions are associated with clinical RAL/ELV resistance mutations. MB-76 directly contacts PFV IN only at the conserved residues P214 and Q215 (P145 and Q146 in HIV IN). (D) Stereoimage showing a superposition of the WT PFV intasome co-crystal structures of DTG (cyan), RAL (magenta), ELV (gray), the recently published XZ-259 (yellow), and MB-76 (green) with Mg^{2+} (PDB IDs 3S3M, 3OYA, 3L2U, 4BE2, and 4IKF respectively). Only the INSTIs and active site Mg^{2+} ions are shown. MB-76 fulfills the common INSTI pharmacophore; positions of the chelating oxygen atoms (O1, O2, and O3) and halobenzyl moiety are largely similar to those observed with other INSTIs. The MB-76 bite angles approach 90°, which is ideal for the octahedral arrangement around the Mg^{2+} ions.

original EC_{50} value and yet the virus failed to break through. Nevertheless, we continued the selection for over 15 months (100 passages) by slowly increasing the concentration of MB-76 (Figure 2A). The viruses selected remained sensitive to MB-76 in the MTT/MT-4 phenotypic assay (Figure 2B). Although sequencing of the genomic DNA extracted at different intervals consistently identified two amino acid substitutions (A128T and V234I) within the IN-coding region, these substitutions were not associated with phenotypic resistance (Figure 2B). No mutations were detected in the RT or Env coding regions nor in the long terminal repeats (LTRs).

MB-76 Binds to the Active Site of PFV IN. In order to gain further insights into the exact molecular mechanism and resistance profile of MB-76, we studied its interaction with the prototype foamy virus (PFV) intasome complex. In contrast to HIV IN, the related PFV IN has proven to be highly amenable to structural studies, culminating in the solution of the PFV intasome structure in 2010 by Hare et al.[14] This complex, consisting of four monomers of the spumaretroviral PFV IN bound to the two cognate viral LTR ends, represents the essential molecular machine that inserts the viral DNA into the host cell chromatin. Importantly, the intasome constitutes the IN assembly required for interaction with INSTIs. Despite a low degree of sequence homology with HIV-1 IN, structural homology is very strong, especially around the active site, allowing extrapolation of findings to other retroviral INs.[14,15] We have hence purified and assembled PFV intasome complexes (Supplementary Figure S2) and evaluated whether the PFV intasome is susceptible to ST inhibition by MB-76. Both RAL and MB-76 were able to block insertion of the oligos into the target plasmid, showing that MB-76 is indeed able to bind and inhibit the PFV intasome (Supplementary Figure S3).

dx.doi.org/10.1021/cb4000426 | *ACS Chem. Biol.* 2013, 8, 1187–1194

Next, we determined the crystal structure of MB-76 bound to the PFV intasome complex (Supplementary Table S1). Our structure reveals, in atomic detail, interactions of MB-76 with the retroviral IN active site. The binding mode of MB-76 is in essence similar to that of INSTIs reported before and involves an induced fit at the two active sites of the enzyme complex (Figure 2C,D).[14−16] The 3′ deoxyadenosine nucleotide (A17) is dislodged upon binding of the inhibitor, effectively disarming the intasome. The MB-76 *p*-fluorobenzyl group assumes the position of the adenine base while the HID core oxygen atoms coordinate Mg^{2+} ions A and B with bite angles approaching the octahedrally ideal 90°, precluding both productive target DNA binding and coordination/activation of the deoxyribose 3′ OH of the viral DNA. In detail, the *p*-fluorobenzyl group makes extensive van der Waals interactions with conserved residues P214 and Q215 (HIV equivalents P145, Q146), the invariant CA dinucleotide, and the guanosine 4 base from the nontransferred strand. Parallel $\pi-\pi$ stacking of the *p*-fluorobenzyl group against the 3′ penultimate cytosine base likely also contributes to the binding free energy of the inhibitor.

At the same time, the electron density suggests that the MB-76 is present in its planar enol form (Supplementary Figures S1B and S4). The HID scaffold has indeed been shown to enolize readily upon Mg^{2+} chelation, both in solution and in the solid state.[18,19] Tautomerization increases the electron density on the carbonyl oxygen atoms, which is favorable for coordination to the active site metal ions. Additionally, since the hydroxyl imide group has a pK_a of ∼8,[19] we can reasonably assume that the bound inhibitor is a dianion (Supplementary Figure S1C). Steric constraints would indeed require both the enol and hydroxylimide oxygen atoms to be deprotonated when bound to the active site Mg^{2+} ions.

Quantum Chemical Analysis of MB-76. Quantum chemical and NMR studies have suggested further aromatization of the enol form of the HID scaffold through delocalization of the nitrogen lone pair, increasing electron density on the C_1-oxo group as well (Supplementary Figure S1B).[19] Similar motifs where a heterocyclic nitrogen lone pair allows aromatization of the ring and concomitantly increases electron density on an attached oxo group can be found in most potent INSTIs (e.g., RAL, ELV, DTG, MK-2048, MK-0536) (Supplementary Figure S5). To acquire additional insights, we have performed theoretical calculations on MB-76 and various other INSTIs using Density Functional Theory (DFT) at the B3LYP/6-311++G(d,p) level of theory (Supplementary Table S2). Natural Bond Orbital (NBO) and Natural Population Analyses (NPA) were performed, shedding light on the electron density distribution in the molecules. As Mg^{2+} is a hard Lewis acid and $=O$ (or $-O^-$) a hard Lewis base, bonding between them is expected to be mainly electrostatically driven. However, significant contributions from nonelectrostatic effects like charge transfer and polarization have been reported for Mg^{2+}−O-ligand complexes.[31,32] Taking this into consideration, we calculated natural partial charges on the three chelating oxygen atoms (q_1, q_2, and q_3), but also their nucleophilicity in electron transfer reactions (as condensed to atom Fukui indices f_{O1}^-, f_{O2}^-, f_{O3}^-) and the isotropic polarizability (Supplementary Table S2). The values obtained are all in the same range, and MB-76 appears to match up to other potent INSTIs in these calculations (Supplementary Table S2).

Characteristics of MB-76 Binding. On the basis of the crystal structure and the chemical data, we can hypothesize that the lack of cross-resistance or resistance development is a result of the unique HID scaffold. This core is very size-efficient in correctly displaying all three oxygen atoms from a single ring and bestowing them with an electronic configuration highly suited for chelation (Supplementary Figure S1C and Table S2). The second, fused ring provides space for further substitution and modulation of physicochemical properties. As such, the scaffold is compact and the only direct contacts being made with PFV IN are with the highly conserved P214 and Q215 residues (P145 and Q146 in HIV-1) (Figure 2C). However, the major resistance mutations N155H and Q148HRK/G140SA are not in direct contact with bound INSTIs. Instead of sterically displacing the inhibitor, they have been shown to slightly detune the IN active site by interfering with Mg^{2+} coordination at either position A or B (in the case of G140/Q148 or N155, respectively, Figure 2C).[15] The INSTI-resistant active site hence demands an additional (re)organization step in order to bind the inhibitor. This accommodation step is likely associated with significant enthalpic/entropic costs, effectively nibbling away at the inhibitors' binding free energy and lowering their potency.[15] It is not entirely clear why MB-76 is insensitive to these active site-distorting resistance mutants or to E92Q. It is likely that various factors contribute to the observed phenotypes. As suggested by Hare *et al*, a highly optimized inhibitor may still tip the scales in favor of binding.[15] MB-76's dianionic character may result in stronger electrostatic interactions while charge transfer from the chelating oxygen atoms can effectively reduce the high charge density on the Mg^{2+} ions, leading to a more stable complex. Finally, also polarization effects can contribute to the binding free energy.[31] Optimal chelation properties, such as the MB-76 ∼90° bite angles, result in an increased energy barrier for ligand dissociation and may (at least partially) lie at the basis of the lower dissociation rates observed for second-generation INSTIs (MK-2048, DTG) compared to ELV and RAL. Slower dissociation was also associated with reduced resistance development.[33] Additionally, the 3′ terminal adenosine nucleotide (A17) has been observed to occupy multiple positions in co-crystal structures with INSTIs, and most are likely non-permissive for inhibitor dissociation. Of interest here may be a conformation in which the adenine base stacks against the ring system carrying the metal coordinating groups. As the presence of this adenosine has been directly linked to inhibitor dissociation, optimizing van der Waals and stacking interactions with this conserved part may further improve ligand characteristics. In our crystal structure we observed clear additional electron density in front of the HID core, which can be explained by an efficiently stacked adenine (Supplementary Figure S4). Like DTG, MB-76 makes use of a longer exocyclic linker between its Mg^{2+}-chelating scaffold and halobenzyl group.[16] Despite the restraints imposed by the amide bond in the linker, this feature endows the compounds with additional flexibility. In turn this can allow them to adopt slightly different positions or conformations in response to a perturbed, resistant active site (the so-called wiggle and jiggle).

Of note, although not tested here, MB-76 does not approach G118 (PFV G187), a site of resistance mutations (G118R) observed with second-generation inhibitors MK-2048 and DTG.[16,34] It is hence possible that MB-76 is less susceptible to substitutions at this position.

dx.doi.org/10.1021/cb4000426 | *ACS Chem. Biol.* 2013, 8, 1187−1194

Drug Combination. Highly active antiretroviral therapy is based on combinations of drugs targeting different stages of the viral life cycle. It is therefore critical that novel antiretrovirals are not antagonistic with drugs in the same or other mechanistic classes. As INSTIs most likely will become an integral part of HAART in the future, it is of particular interest to study combinations of novel INSTIs with RT inhibitors to rule out antagonism. Using MacSynergy II,[35] we studied the impact of combining MB-76 with INSTIs and RT inhibitors. Combinations to control for synergy (didanosine + ribavirin), antagonism (AZT + ribavirin), and Loewe additivity (RAL + RAL) were included in the study (Figure 3). Combination of

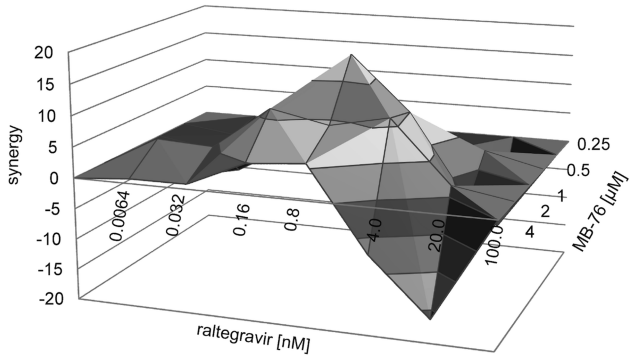

	Synergy/antagonism at 95%CI	
combination	synergy	antagonism
rbv+AZT	48,9+/-8,4	-471,6+/-222,6
rbv+DDI	353,1+/-30,5	-19,5+/-14,9
ral+ral	91,3+/-16,6	-31,7+/-27,2
ral+evg	124,5+/-23,6	-85,2+/-43,8
MB-76+ral	149,5+/-57,5	-57,9+/-12,4
MB-76+AZT	203,9+/-19,7	-46,4+/-6,3

Figure 3. MacSynergyII analysis of the anti-HIV-1 activity of MB-76 in combination with AZT and RAL. (A) Representative synergy plot for the combination of MB-76 and RAL at different concentrations. (B) Results of the MacSynergyII analyses for different drug combinations. Synergy volumes (volume above or below the surface in μM^2) with 95% confidence interval as calculated by MacSynergyII are shown. Strongly synergistic or antagonistic interactions result in a large positive or negative volume respectively. Values are calculated from at least two independent experiments, each having 5 parallel wells. The values obtained for the different combinations are interpreted as follows: ribavirin + AZT, antagonism; ribavirin + didanosine, synergy; RAL + RAL, ELV, or MB-76, (Loewe) additivity; MB-76 + AZT, (Bliss independence-type) additivity to synergism.

RAL with MB-76 generally resulted in additive effects. As expected, highly similar values were observed for the RAL + MB-76 combination and the RAL + ELV combination. Loewe additivity had been reported previously when combining the two INSTIs RAL and ELV.[36] As RT and integration inhibitors act on different targets but inhibition of the first target directly influences the second, combining them should lead to more Bliss independence-type additive effects. Indeed, combination of MB-76 and AZT yielded additive or slightly synergistic effects.

Detailed Analysis of MB-76 Toxicity and Metabolism. To evaluate the potential of a novel drug to proceed into preclinical development, cellular toxicity and metabolism ought to be investigated. The cytochrome P450 (CYP) is a large superfamily of enzymes involved in drug metabolism via oxidation of organic substances. Changes in the activity or expression levels of CYPs are the major source of adverse effects of drugs. Therefore potential inhibition of members of the CYP pathway should be analyzed carefully during lead optimization. As shown in Supplementary Table S3, MB-76 only faintly inhibited the different CYPs tested (CYP1A2, CYP2C9, CYP2C19, CYP2D6, and CYP3A4). At a concentration of 10 μM MB-76 did not block any of the CYPs for 50%, and for three out of five CYPs inhibition was even below 10%. Known CYP inhibitors analyzed in parallel produced IC_{50} values in the low and submicromolar range. In addition an extended study on the toxicity of this compound was performed (Supplementary Tables S4 and S5). First the effects on cell number, intracellular free calcium, nuclear size, membrane permeability, and mitochondrial potential were measured. MB-76 did not display any severe toxicity in these assays even at high concentrations of 100 μM. The control compound, cerivastatin, in contrast potently induced cellular toxicity with an IC_{50} in the submicromolar range. Concurrently, MB-76 did not significantly inhibit hERG (human Ether-a-go-go-Related Gene potassium channel 1), a cardiac potassium channel that plays a critical role in defining ventricular repolarization. Non-cardiovascular drugs associated with ventricular arrhythmia have been linked to delayed cardiac repolarization and lowering of the hERG current. As expected the control compound E-4031 induced hERG-mediated cardiac toxicity with an IC_{50} in the low nanomolar range. Taking all data together we can conclude that in the assays tested so far MB-76 does not give any reason for concern regarding toxicity or metabolism. During further lead optimization a more thorough analysis and a complete ADMETox (absorption/administration, distribution, metabolism, excretion/elimination, and toxicity) profile will be necessary to evaluate the potential of this novel class of compounds to proceed further into preclinical development.

Conclusion. As INSTIs have become an integral part of HAART, it will be of crucial importance to develop treatment options for patients failing on first generation inhibitors such as RAL or ELV. The lack of cross-resistance, the failure of resistance selection due to its unique molecular properties, the low toxicity, and favorable metabolism support further clinical development of HIDs as second generation IN inhibitors.

METHODS

Time of Addition. MT-4 cells (100,000 per well) in a 96-well microtiter plate were infected with HIV-IIIB at an MOI (multiplicity of infection) of 0.7. Compounds were added at different time points after infection (1, 2, 3, 4, 5, 6, 7, 8, 9, 10, 11, 12, 24, and 25 h) as described previously.[37] Viral p24 antigen production was determined 30 h postinfection by ELISA (Innogenetics). Compounds were added at 50 and 100 times their EC_{50} as determined by the MTT/MT-4 assay.

Quantification of Different HIV-1 DNA Species during HIV Infection by Real-Time PCR. HeLaP4 cells (1×10^6 cells per well in a 6-well plate) were infected with HIV-1 IIIB (equivalent of 1 μg of p24) in the absence or presence of the test compounds. After 2 h of incubation at 37 °C the cells were washed 3 times with phosphate-buffered saline. When infection medium was replaced with new medium, fresh inhibitors were added. In each 6-well plate, uninfected HeLaP4 cells were incubated in parallel. DNA extractions and quantification of late reverse transcripts, two-long terminal repeat (2-LTR) circles, and integrants were done as described earlier.[38]

Resistance Selection. Resistance selection of HIV-1 NL4.3 against MB-76 was initiated at a low MOI (MOI = 0.01) in MT-4 and C8166 cells in parallel in a 24-well plate format and at a drug concentration of 2 μM. Every 3 to 4 days the cell culture was monitored for the appearance of an HIV-induced CPE. When CPE was observed, the cell-free supernatants were used to infect new MT-4 cells in the presence of an equal or 2- to 5-fold higher concentration of the compound. When no CPE was observed, the cells were subcultured in the presence of the same concentration of the compound. The experiment was performed for over 15 months (100 passages) and was then terminated as the resulting virus still did not show any resistance in the MTT/MT-4 phenotypic assay.

PCR Amplification and Sequencing of the IN- and RT-Coding Region of pol, env, and the LTRs. Proviral DNA extraction of MT-4 cells, infected with HIV-1 NL4.3 grown in the presence of MB-76, was performed using the QIAamp blood kit (Qiagen). PCR amplification and sequencing of the Env-, RT-, and IN-coding regions and LTR sequences was done as described previously.[39] Mutations present in more than 20−25% of the global virus population can be detected by means of population sequencing and sequences are analyzed by comparing with the wild-type strain passaged in parallel.

Drug metabolism and toxicity studies were performed in standard assays by Cerep, France (www.cerep.fr).

■ ASSOCIATED CONTENT

Ⓢ Supporting Information

This material is available free of charge via the Internet at http://pubs.acs.org.

Accession Codes

Coordinates and associated structure factors of MB-76 bound to the PFV intasome have been deposited in the Protein Data Bank with ID 4IKF.

■ AUTHOR INFORMATION

Corresponding Author

*E-mail: frauke.christ@med.kuleuven.be.

Author Contributions

‖These authors contributed equally to this work.

Author Contributions

⊥These authors contributed equally to this work.

Notes

The authors declare no competing financial interest.

■ ACKNOWLEDGMENTS

We are grateful to B. Van Remoortel, N. J. Van der Veken, and L. Desender for excellent technical assistance. Research was funded by the OT and the IOF Program of the KU Leuven, the EU-funded project CHAARM (HEALTH-F3-2009-242135), grants from the Ministère de l'Enseignement Supérieur et de la Recherche Française, the Centre National de la Recherche Scientifique (CNRS), and the Agence Nationale de la Recherche contre le Sida (ANRS). F.C. is an IOF fellow, J.D. is a doctoral fellow for the Research Foundation−Flanders (FWO), and B.A.D. is a DBOF fellow of the KU Leuven. We extend thanks to P. Cherepanov for the PFV expression constructs and detailed protocols and to C. Calmels and ML. Andréola for the RNase H data.

■ REFERENCES

(1) Summa, V., Petrocchi, A., Bonelli, F., Crescenzi, B., Donghi, M., Ferrara, M., Fiore, F., Gardelli, C., Gonzalez Paz, O., Hazuda, D. J., Jones, P., Kinzel, O., Laufer, R., Monteagudo, E., Muraglia, E., Nizi, E., Orvieto, F., Pace, P., Pescatore, G., Scarpelli, R., Stillmock, K., Witmer, M. V., and Rowley, M. (2008) Discovery of raltegravir, a potent, selective orally bioavailable HIV-integrase inhibitor for the treatment of HIV-AIDS infection. *J. Med. Chem. 51*, 5843−5855.

(2) Neamati, N. (2011) HIV-1 Integrase Inhibitor Design: Overview and Historical Perspectives, in *HIV-1 Integrase: Mechanism and Inhibitor Design* (Neamati, N., Ed.), pp 165−196, John Wiley & Sons, Inc., Hoboken, NJ.

(3) Christ, F., Thys, W., De Rijck, J., Gijsbers, R., Albanese, A., Arosio, D., Emiliani, S., Rain, J.-C., Benarous, R., Cereseto, A., and Debyser, Z. (2008) Transportin-SR2 imports HIV into the nucleus. *Curr. Biol. 18*, 1192−1202.

(4) Lewinski, M. K., Yamashita, M., Emerman, M., Ciuffi, A., Marshall, H., Crawford, G., Collins, F., Shinn, P., Leipzig, J., Hannenhalli, S., Berry, C. C., Ecker, J. R., and Bushman, F. D. (2006) Retroviral DNA integration: viral and cellular determinants of target-site selection. *PLoS Pathog. 2*, e60.

(5) Wang, G. P., Ciuffi, A., Leipzig, J., Berry, C. C., and Bushman, F. D. (2007) HIV integration site selection: analysis by massively parallel pyrosequencing reveals association with epigenetic modifications. *Genome Res. 17*, 1186−1194.

(6) Schrijvers, R., De Rijck, J., Demeulemeester, J., Adachi, N., Vets, S., Ronen, K., Christ, F., Bushman, F. D., Debyser, Z., and Gijsbers, R. (2012) LEDGF/p75-independent HIV-1 replication demonstrates a role for HRP-2 and remains sensitive to inhibition by LEDGINs. *PLoS Pathog. 8*, No. e1002558.

(7) Murray, J. M., Emery, S., Kelleher, A. D., Law, M., Chen, J., Hazuda, D. J., Nguyen, B. Y. T., Teppler, H., and Cooper, D. A. (2007) Antiretroviral therapy with the integrase inhibitor raltegravir alters decay kinetics of HIV, significantly reducing the second phase. *AIDS 21*, 2315−2321.

(8) Malet, I., Delelis, O., Valantin, M.-A., Montes, B., Soulie, C., Wirden, M., Tchertanov, L., Peytavin, G., Reynes, J., Mouscadet, J.-F., Katlama, C., Calvez, V., and Marcelin, A.-G. (2008) Mutations associated with failure of raltegravir treatment affect integrase sensitivity to the inhibitor in vitro. *Antimicrob. Agents Chemother. 52*, 1351−1358.

(9) Zolopa, A. R., Berger, D. S., Lampiris, H., Zhong, L., Chuck, S. L., Enejosa, J. V., Kearney, B. P., and Cheng, A. K. (2010) Activity of elvitegravir, a once-daily integrase inhibitor, against resistant HIV Type 1: results of a phase 2, randomized, controlled, dose-ranging clinical trial. *J. Infect. Dis. 201*, 814−822.

(10) Molina, J.-M., Lamarca, A., Andrade-Villanueva, J., Clotet, B., Clumeck, N., Liu, Y.-P., Zhong, L., Margot, N., Cheng, A. K., Chuck, S. L., and Study 145 Team (2012) Efficacy and safety of once daily elvitegravir versus twice daily raltegravir in treatment-experienced patients with HIV-1 receiving a ritonavir-boosted protease inhibitor: randomised, double-blind, phase 3, non-inferiority study. *Lancet Infect. Dis. 12*, 27−35.

(11) Min, S., Sloan, L., DeJesus, E., Hawkins, T., McCurdy, L., Song, I., Stroder, R., Chen, S., Underwood, M., Fujiwara, T., Piscitelli, S., and Lalezari, J. (2011) Antiviral activity, safety, and pharmacokinetics/pharmacodynamics of dolutegravir as 10-day monotherapy in HIV-1-infected adults. *AIDS 25*, 1737−1745.

(12) Underwood, M. R., Johns, B. A., Sato, A., Martin, J. N., Deeks, S. G., and Fujiwara, T. (2012) The activity of the integrase inhibitor dolutegravir against HIV-1 variants isolated from raltegravir-treated adults. *J. Acquired Immune Defic. Syndr. 61*, 297−301.

(13) Canducci, F., Ceresola, E. R., Boeri, E., Spagnuolo, V., Cossarini, F., Castagna, A., Lazzarin, A., and Clementi, M. (2011) Cross-resistance profile of the novel integrase inhibitor Dolutegravir (S/GSK1349572) using clonal viral variants selected in patients failing raltegravir. *J. Infect. Dis. 204*, 1811−1815.

(14) Hare, S., Gupta, S. S., Valkov, E., Engelman, A., and Cherepanov, P. (2010) Retroviral intasome assembly and inhibition of DNA strand transfer. *Nature 464*, 232−236.

(15) Hare, S., Vos, A. M., Clayton, R. F., Thuring, J. W., Cummings, M. D., and Cherepanov, P. (2010) Molecular mechanisms of retroviral integrase inhibition and the evolution of viral resistance. *Proc. Natl. Acad. Sci. U.S.A. 107*, 20057−20062.

(16) Hare, S., Smith, S. J., Métifiot, M., Jaxa-Chamiec, A., Pommier, Y., Hughes, S. H., and Cherepanov, P. (2011) Structural and functional analyses of the second-generation integrase strand transfer inhibitor dolutegravir (S/GSK1349572). *Mol. Pharmacol. 80*, 565−572.
(17) Marinello, J., Marchand, C., Mott, B. T., Bain, A., Thomas, C. J., and Pommier, Y. (2008) Comparison of raltegravir and elvitegravir on HIV-1 integrase catalytic reactions and on a series of drug-resistant integrase mutants. *Biochemistry 47*, 9345−9354.
(18) Billamboz, M., Bailly, F., Lion, C., Calmels, C., Andréola, M.-L., Witvrouw, M., Christ, F., Debyser, Z., De Luca, L., Chimirri, A., and Cotelle, P. (2011) 2-Hydroxyisoquinoline-1,3(2H,4H)-diones as inhibitors of HIV-1 integrase and reverse transcriptase RNase H domain: influence of the alkylation of position 4. *Eur. J. Med. Chem. 46*, 535−546.
(19) Billamboz, M., Bailly, F., Lion, C., Touati, N., Vezin, H., Calmels, C., Andréola, M.-L., Christ, F., Debyser, Z., and Cotelle, P. (2011) Magnesium chelating 2-hydroxyisoquinoline-1,3(2H,4H)-diones, as inhibitors of HIV-1 integrase and/or the HIV-1 reverse transcriptase ribonuclease H domain: discovery of a novel selective inhibitor of the ribonuclease H function. *J. Med. Chem. 54*, 1812−1824.
(20) Debyser, Z., Cherepanov, P., Van Maele, B., De Clercq, E., and Witvrouw, M. (2002) In search of authentic inhibitors of HIV-1 integration. *Antiviral Chem. Chemother. 13*, 1−15.
(21) Christ, F., Voet, A., Marchand, A., Nicolet, S., Desimmie, B. A., Marchand, D., Bardiot, D., Van Der Veken, N. J., Van Remoortel, B., Strelkov, S. V., De Maeyer, M., Chaltin, P., and Debyser, Z. (2010) Rational design of small-molecule inhibitors of the LEDGF/p75-integrase interaction and HIV replication. *Nat. Chem. Biol. 6*, 442−448.
(22) Hazuda, D. J., Felock, P., Witmer, M., Wolfe, A., Stillmock, K., Grobler, J. A., Espeseth, A., Gabryelski, L., Schleif, W., Blau, C., and Miller, M. D. (2000) Inhibitors of strand transfer that prevent integration and inhibit HIV-1 replication in cells. *Science 287*, 646−650.
(23) Daelemans, D., Pauwels, R., De Clercq, E., and Pannecouque, C. (2011) A time-of-drug addition approach to target identification of antiviral compounds. *Nat. Protoc. 6*, 925−933.
(24) Christ, F., Shaw, S., Demeulemeester, J., Desimmie, B. A., Marchand, A., Butler, S., Smets, W., Chaltin, P., Westby, M., Debyser, Z., and Pickford, C. (2012) Small-molecule inhibitors of the LEDGF/p75 binding site of integrase block HIV replication and modulate integrase multimerization. *Antimicrob. Agents Chemother. 56*, 4365−4374.
(25) Delelis, O., Malet, I., Na, L., Tchertanov, L., Calvez, V., Marcelin, A.-G., Subra, F., Deprez, E., and Mouscadet, J.-F. (2009) The G140S mutation in HIV integrases from raltegravir-resistant patients rescues catalytic defect due to the resistance Q148H mutation. *Nucleic Acids Res. 37*, 1193−1201.
(26) Larder, B. A., Chesebro, B., and Richman, D. D. (1990) Susceptibilities of zidovudine-susceptible and -resistant human immunodeficiency virus isolates to antiviral agents determined by using a quantitative plaque reduction assay. *Antimicrob. Agents Chemother. 34*, 436−441.
(27) Nunberg, J. H., Schleif, W. A., Boots, E. J., O'Brien, J. A., Quintero, J. C., Hoffman, J. M., Emini, E. A., and Goldman, M. E. (1991) Viral resistance to human immunodeficiency virus type 1-specific pyridinone reverse transcriptase inhibitors. *J. Virol. 65*, 4887−4892.
(28) De Vreese, K., Reymen, D., Griffin, P., Steinkasserer, A., Werner, G., Bridger, G. J., Esté, J., James, W., Henson, G. W., Desmyter, J., Anné, J., and De Clercq, I. (1996) The bicyclams, a new class of potent human immunodeficiency virus inhibitors, block viral entry after binding. *Antiviral Res. 29*, 209−219.
(29) Métifiot, M., Maddali, K., Johnson, B. C., Hare, S., Smith, S. J., Zhao, X. Z., Marchand, C., Burke, T. R., Hughes, S. H., Cherepanov, P., and Pommier, Y. (2013) Activities, crystal structures, and molecular dynamics of dihydro-1H-isoindole derivatives, inhibitors of HIV-1 integrase. *ACS Chem. Biol. 8*, 209−217.
(30) Johnson, V. A., Brun-Vézinet, F., Clotet, B., Günthard, H. F., Kuritzkes, D. R., Pillay, D., Schapiro, J. M., and Richman, D. D. (2007) Update of the drug resistance mutations in HIV-1: 2007. *Top HIV Med. 15*, 119−125.
(31) Petrov, A. S., Bowman, J. C., Harvey, S. C., and Williams, L. D. (2011) Bidentate RNA-magnesium clamps: on the origin of the special role of magnesium in RNA folding. *RNA 17*, 291−297.
(32) Solt, I., Simon, I., Császár, A. G., and Fuxreiter, M. (2007) Electrostatic versus nonelectrostatic effects in DNA sequence discrimination by divalent ions Mg2+ and Mn2+. *J. Phys. Chem. B 111*, 6272−6279.
(33) Hightower, K. E., Wang, R., Deanda, F., Johns, B. A., Weaver, K., Shen, Y., Tomberlin, G. H., Carter, H. L., Broderick, T., Sigethy, S., Seki, T., Kobayashi, M., and Underwood, M. R. (2011) Dolutegravir (S/GSK1349572) exhibits significantly slower dissociation than raltegravir and elvitegravir from wild type and integrase inhibitor-resistant HIV-1 integrase-DNA complexes. *Antimicrob. Agents Chemother. 55*, 4552−4559.
(34) Bar-Magen, T., Sloan, R. D., Donahue, D. A., Kuhl, B. D., Zabeida, A., Xu, H., Oliveira, M., Hazuda, D. J., and Wainberg, M. A. (2010) Identification of novel mutations responsible for resistance to MK-2048, a second-generation HIV-1 integrase inhibitor. *J. Virol. 84*, 9210−9216.
(35) Prichard, M. N., and Shipman, C. (1990) A three-dimensional model to analyze drug-drug interactions. *Antiviral Res. 14*, 181−205.
(36) Jilek, B. L., Zarr, M., Sampah, M. E., Rabi, S. A., Bullen, C. K., Lai, J., Shen, L., and Siliciano, R. F. (2012) A quantitative basis for antiretroviral therapy for HIV-1 infection. *Nat. Med. 18*, 446−451.
(37) Pauwels, R., Andries, K., Desmyter, J., Schols, D., Kukla, M. J., Breslin, H. J., Raeymaeckers, A., Van Gelder, J., Woestenborghs, R., and Heykants, J. (1990) Potent and selective inhibition of HIV-1 replication in vitro by a novel series of TIBO derivatives. *Nature 343*, 470−474.
(38) Van Maele, B., De Rijck, J., De Clercq, E., and Debyser, Z. (2003) Impact of the central polypurine tract on the kinetics of human immunodeficiency virus type 1 vector transduction. *J. Virol. 77*, 4685−4694.
(39) Hombrouck, A., Hantson, A., Van Remoortel, B., Michiels, M., Vercammen, J., Rhodes, D., Tetz, V., Engelborghs, Y., Christ, F., Debyser, Z., and Witvrouw, M. (2007) Selection of human immunodeficiency virus type 1 resistance against the pyranodipyrimidine V-165 points to a multimodal mechanism of action. *J. Antimicrob. Chemother. 59*, 1084−1095.